VILNIUS UNIVERSITY

CENTER FOR PHYSICAL SCIENCES AND TECHNOLOGY

Tadas Mineikis

# Stochastic galaxy disk evolution. 2-D models

Vilnius, 2015

VILNIAUS UNIVERSITETAS

FIZINIŲ IR TECHNOLOGIJOS MOKSLŲ CENTRAS

Tadas Mineikis

# Stochastinė galaktikų diskų evoliucija. 2-D modeliai

Daktaro disertacijos santrauka

Fiziniai mokslai, fizika (02 P)

Vilnius, 2015

Disertacija parengta 2010–2014 metais Vilniaus universitete.

Mokslinis vadovas –
Prof. dr. Vladas Vansevičius (Vilniaus universitetas, fiziniai mokslai, fizika – 02 P)

Disertacija ginama Vilniaus universiteto Fizikos mokslo krypties taryboje:

Pirmininkas –
dr. Arūnas Kučinskas (Vilniaus universitetas, fiziniai mokslai, fizika – 02 P)

Nariai:

Dr. Vidas Dobrovolskas (Vilniaus universitetas, fiziniai mokslai, fizika – 02 P)

Dr. Julius Sperauskas (Vilniaus universitetas, fiziniai mokslai, fizika – 02 P)

Dr. Laimons Začs (Latvijos universitetas, fiziniai mokslai, fizika – 02 P)

Dr. Kastytis Zubovas (Fizinių ir technologijos mokslų centras, fiziniai mokslai, fizika – 02 P)

Disertacija bus ginama viešame Fizikos mokslo krypties tarybos posėdyje 2015 m. rugsėjo 23 d. 14:00 Vilniaus universiteto Astronomijos observatorijoje.
Adresas: M. K. Čiurlionio 29, LT-03100, Vilnius, Lietuva
Telefonas: (+370-5) 239 8760; Faksas: (+370-5) 239 8767

Disertacijos santrauka išsiutinėta 2015 m. rugpjūčio mėn. 21 d.

Disertacijos santrauka yra Vilniaus universiteto ir Fizinių ir technologijos mokslų centro bibliotekose bei interneto svetainėje adresu:
www.vu.lt/lt/naujienos/ivykiu-kalendorius

# Motivation

The Universe is a huge scientific laboratory available for the human kind; however in order to properly use it, we must understand how it works. In the last century our knowledge of the Universe dramatically expanded. This leap was possible thanks to increased capabilities of observational techniques and theoretical methods. However, despite ongoing efforts we still are lacking a proper understanding of the crucial process in the Universe – star formation in galaxies.

Due to extreme space and time scales usually present in galaxies scientists cannot rely on controlled experiments to study astrophysical phenomena. For this reason, studies of star formation rely heavily on theoretical models. Theoretical models allow us to make virtual experiments, predict observational features, and, if they are confirmed, trust that our simulations reflect the reality properly.

For the most advanced numerical models of galaxy formation and evolution the hydrodynamical/N-body methods are used for simulations. However, this approach currently faces some difficulties. It is computationally highly costly, strongly dependent on the parameterization of the sub-grid physics, and even on the implementation methods (Scannapieco et al. 2012). Additionally, in the case of late-type spiral galaxy simulations, fine tuning of the models is needed (Roškar et al. 2014, and references therein). An increased spatial resolution of the simulations could be the key to the problem (Guedes et al. 2011), however, this would make galaxy models computationally even more daunting. Due to these reasons the hydrodynamical/N-body models are still not very effective for the analysis and interpretation of star formation data in the cases of resolved disk galaxies.

Other approaches to study star formation in galaxies use semi-analytical models, e.g., Kang et al. (2012). The semi-analytical models describe various processes in galaxies mainly via analytical expressions. Therefore, the models are very fast to compute, but include a large number of free parameters. Additionally, semi-analytical models are exclusively one dimensional (1-D – resolved along the radius of a galaxy), therefore, they are of limited use in the space-resolved studies of star formation histories.

In this thesis we present a new model for simulations of star formation in galaxy disks. Simulations of 2-D disks allow us to predict a wide range of observational features and make our model a useful tool for studies of star formation in disk galaxies.

## Aim of the study

Study the impact of stochastic star formation on the evolution of galaxy disks.

## Main tasks

1. Build a 2-D galaxy disk model driven by stochastic star formation.

2. Develop a software package for galaxy disk modeling.

3. Study the star formation history of the M33 galaxy.

## Main results and statements to defend

1. The proposed stochastic 2-D galaxy disk evolution model reproduces well the parameter range of the late-type galaxy disks.

2. The software package, developed to model galaxy disk evolution, can produce simulated observation data of the resolved and unresolved stellar populations in any arbitrary spectrophotometric system.

3. The proper account for the effects of stochastic star formation is required in order to derive accurate parameters of the late-type galaxy disks.

4. The derived parameters of the M33 galaxy disk: triggered star formation probability $P_{\mathrm{T}} = 0.34$, star formation efficiency $\epsilon = 0.2\,\%$, and metal-enriched gas outflow $\eta = 0.9$.

## Publications on thesis topic in refereed journals

1. **Mineikis T.**, Vansevičius V. 2010, *Disk galaxy models driven by stochastic self-propagating star formation //* Baltic Astronomy, 19, 111
2. **Mineikis T.**, Vansevičius V. 2014, *Stochastic 2-D models of galaxy disk evolution. The galaxy M33 //* Baltic Astronomy, 23, 209
3. **Mineikis T.**, Vansevičius V. 2014, *Models of late-type disk galaxies: 1-D versus 2-D //* Baltic Astronomy, 23, 221
4. **Mineikis T.**, Vansevičius V. 2015, *Stochastic 2-D galaxy disk evolution models. Resolved stellar populations in the galaxy M33 //* Baltic Astronomy, 24, 223

## Other publications in refereed journals

1. de Meulenaer P., Narbutis D., **Mineikis T.**, Vansevičius V. 2013, *Deriving physical parameters of unresolved star clusters. I. Age, mass, and extinction degeneracies* // A&A, 550, A20

2. de Meulenaer P., Narbutis D., **Mineikis T.**, Vansevičius V. 2014, *Deriving physical parameters of unresolved star clusters. II. The degeneracies of age, mass, extinction, and metallicity* // A&A, 569, A4

3. de Meulenaer P., Narbutis D., **Mineikis T.**, Vansevičius V. 2014, *Stochasticity in star clusters: reduced random sampling method* // Baltic Astronomy, 23, 199

4. Narbutis D., Semionov D., Stonkutė R., de Meulenaer P., **Mineikis T.**, Bridžius A., Vansevičius V. 2014, *Deriving structural parameters of semi-resolved star clusters. FitClust: a program for crowded fields* // A&A, 569, A30

5. Narbutis D., Stonkutė R., de Meulenaer P., **Mineikis T.**, Vansevičius V. 2014, *Structural parameters of star clusters: stochastic effects* // Baltic Astronomy, 23, 103

6. de Meulenaer P., Narbutis D., **Mineikis T.**, Vansevičius V. 2015, *Deriving physical parameters of unresolved star clusters. III. Application to M 31 PHAT clusters* // A&A, 574, A66

## Presentations at conferences

1. **Mineikis T.**, Vansevičius V. *Disk evolution of the spiral galaxy M33* // "4th Conference of Lithuanian astronomical union. Space science yesterday, today and tomorrow.", Vilnius (Lithuania), June 13, 2008 (oral presentation)

2. **Mineikis T.**, Vansevičius V. *Stochastic galaxy disk model* // "38th Lithuanian national conference of physics", Vilnius (Lithuania), June 8-10, 2009 (poster presentation)

3. **Mineikis T.**, Vansevičius V. *GALEMO: disky galaxies evolution model* // "39th Lithuanian national conference of physics", Vilnius (Lithuania), October 6-8, 2011 (poster presentation)

4. **Mineikis T.**, Vansevičius V. *Models of late type galaxy evolution: 1D versus 2D* // "European week of astronomy and space science", Turku (Finland), July 8-12, 2013 (oral presentation)

5. **Mineikis T.**, Vansevičius V. *Stochastic 2-D galaxy disk evolution modeling. The M33 galaxy //* "Physical processes of galaxy formation: consensus and challenges", Aix en Provance (France), July 22-26, 2013 (poster presentation)

## Personal contribution

The author together with the scientific supervisor developed the stochastic 2-D galaxy disk evolution model, analyzed results of simulations, and published 4 main thesis papers. The author implemented the model and auxiliary tools for the simulation of galaxy disks, collected and reduced observational data of the M33 galaxy for the comparison of models with observations. Overall contribution by the author is not less than 70 %.

## Thesis summary outline

In Section 1 we describe our stochastic 2-D galaxy disk evolution model; in Section 2 we apply the model to study the evolution of the M33 galaxy disk; in Section 3 we compare our 2-D model with 1-D galaxy evolution models; the conclusions are presented in the final chapter.

# 1. The model

## 1.1. Disk geometry and time step

The disk model is divided into $N_{\mathrm{R}}$ rings of equal width (Mineikis & Vansevičius 2010). Each ring is subdivided into cells, which are the smallest elements of the model. This subdivision follows the rule that the ring with the running number $i$ has $6 \cdot i$ cells, producing a total of $3N_{\mathrm{R}}(N_{\mathrm{R}} - 1) + 1$ cells in the disk. This subdivision results in equal area cells, except for the central one, which is smaller by a factor of $3/4$. The physical size of the disk model is defined by the physical size of cells and the number of rings.

We assume the size of cells to be comparable to the typical size of OB associations. According to the recent findings by Bastian et al. (2007), star formation (SF) is a hierarchical scale-free process, highly dependent on the definitions. Nevertheless, our model is not very sensitive to the adopted cell size, therefore, in this study, a cell size is set to $d_{\mathrm{C}} = 100$ pc.

The model integration time step ($\Delta t_\mathrm{I}$) corresponds to the SF propagation time across the cell. We assume that the SF propagation velocity is $v_\mathrm{SF} = 10$ km/s (Feitzinger et al. 1981), i.e., it corresponds to the typical speed of sound in the interstellar matter within a cell, therefore:

$$\Delta t_\mathrm{I} = 10 \text{ Myr} \cdot \frac{d_\mathrm{C}}{100 \text{ pc}} \cdot \left(\frac{v_\mathrm{SF}}{10 \text{ km/s}}\right)^{-1}. \tag{1}$$

## 1.2. Gas accretion

Although mass accretion histories of dark matter (DM) halos are highly variable (McBride et al. 2009), they tend, on average, to obey simple relations. McBride et al. (2009) studied the Millennium simulation data and found a simple empirical fit to the average DM accretion rate. The fit relates the mean accretion rate of DM to a given halo mass at a given redshift. Using the higher resolution Millennium II simulation, Fakhouri et al. (2010) confirmed the validity of the fit and extended it to smaller halo masses. We use the results by Fakhouri et al. (2010) to prescribe the DM and, correspondingly, baryonic mass (BM) build-up of the model.

The gas falling into the DM halo is distributed in the thin disk. The radial profile of the accretion is assumed to be a scaled version of the total BM radial profile of the present-day galaxy disk:

$$A_\mathrm{G}(r, t) = \frac{B(r)}{2\pi \int_0^R B(r) r \mathrm{d}r} \cdot A_\mathrm{DM}(t) \cdot \beta, \tag{2}$$

where $A_\mathrm{G}(r, t)$ is the radial profile of gas accretion rate, $B(r)$ is the radial profile of BM density in the galaxy disk, $A_\mathrm{DM}(t)$ is the rate of DM accretion on the galaxy halo, and $\beta = \Omega_\mathrm{BM}/\Omega_\mathrm{DM}$ is the primordial ratio of BM to DM. Such a definition of accretion guarantees the build-up of the present-day disk over the galaxy's life-time. The metallicity of the accreted gas is set to $Z_\mathrm{A} = 0.0001$.

## 1.3. Star formation

The star formation process in the disk is modeled by discrete SF events occurring stochastically in the cells. The cell can experience a SF event spontaneously (probability $P_\mathrm{S}$) or be triggered (probability $P_\mathrm{T}$).

• *Spontaneous SF probability $P_\mathrm{S}$*: this parameter defines SF events occurring stochastically in the cells without any external influence. The spontaneous SF sus-

tains SF activity in the disk. In this study we set $P_{\mathrm{S}}$ to be very small, i.e., $\sim 1$ SF event per model integration time-step $\Delta t_{\mathrm{I}}$ over the whole disk. Additionally, we assume that spontaneous SF events are more probable in the cells possessing higher gas density: $P_{\mathrm{S}} \propto \Sigma_{\mathrm{G}}^2$, where $\Sigma_{\mathrm{G}}$ is a surface gas density within a cell.

  • *Triggered SF probability* $P_{\mathrm{T}}$: this parameter represents a chain of complex processes in the cell's interstellar medium (molecular cloud) after the SF event has occurred. A molecular cloud will undergo imminent disruption by an energetic feedback of stellar winds, expanding H II zones and supernovae explosions. Despite a negative SF feedback locally (on a scale of cell), SF could be triggered on a larger scale (i.e., in neighboring cells). For the cell $i$, which experiences a SF event in a time step $t_k$, the neighboring cell $j$, being in direct contact with the cell $i$, can experience a SF event during the next time step $t_{k+1}$ with a probability of $P_{\mathrm{T},j}$.

At the start of galaxy simulation the SF in the disk is inhibited by the critical gas surface density $\Sigma_{\mathrm{C}}$. If the gas surface density in a cell is below critical, the probability of SF event is reduced by a factor of $\Sigma_{\mathrm{G}}/\Sigma_{\mathrm{C}}$. As the simulation evolves, the gas density in the disk increases and SF becomes more probable starting from the inner disk parts. In the outer disk, $\Sigma_{\mathrm{G}}$ remains small, compared to $\Sigma_{\mathrm{C}}$, for a longer time and defines the extent of the SF disk. We note that $\Sigma_{\mathrm{C}}$ defines the local density, i.e., not averaged azimuthally, as this parameter is usually derived from observations.

During a SF event, a fraction of gas available in a cell is converted to stars. This fraction is called the SF efficiency, SFE:

$$\mathrm{SFE} = \epsilon \cdot \left( \frac{\Sigma_{\mathrm{G}}}{10 \ M_\odot/\mathrm{pc}^2} \right)^\alpha, \tag{3}$$

where $\epsilon$ and $\alpha$ are free parameters. In order to avoid generating unrealistic stellar populations of extremely low mass or SFE exceeding 100%, we set the lower and upper SFE cut-offs to 0.05% and 50%, respectively. Additionally, if the stellar population, born in a cell, is less massive than $100 \, M_\odot$, we assume that the starburst does not trigger neighboring cells because the population is, on average, lacking supernovae.

## 1.4. The evolution of cells

Each stellar population, formed in a cell during a SF event, could be well represented by a simple stellar population (SSP). To track the entire SF history of a cell, the value of mass of each particular stellar population is stored in a 2-D (age vs. metallicity) array, $S$. The step in age, $t_{\mathrm{S}}$, can be set in accordance to the size of a cell (10 Myr

**Table 1.** PEGASE-HR parameters used to generate SSPs.

| Parameter | Value | Reference |
|---|---|---|
| Stellar library | low-resolution | Le Borgne et al. (2004) |
| Initial mass function | corrected for binaries | Kroupa (2002) |
| Fraction of close binaries | 0.05 | default PEGASE-HR value |
| Ejecta of massive stars | type B | Woosley & Weaver (1995) |
| Nebular emission | true | PEGASE-HR value |

throughout the paper). The step in metallicity (0.1–0.3 dex) is predefined by the used dataset of interpolated isochrones. To track the evolution of SSPs self-consistently, we employ the package PEGASE-HR (Le Borgne et al. 2004, see Table 1 for the parameters used).

The stars from any SSP, formed in a cell, can move to the neighboring cell, therefore, arrays $S_j$ of the neighboring cells have to be modified accordingly. Stellar spread to neighboring cells is implemented as a "dispersion" process. The evolution of the stellar content in the cell $S_i$ is given by

$$\frac{\Delta S_i}{\Delta t} = \Psi_i - D_{\mathrm{S}} \cdot \sum_j \lambda_{i,j} \cdot (S_i - S_j), \qquad (4)$$

where $\Psi_i$ is the mass of a newly formed SSP, $D_{\mathrm{S}}$ is the "dispersion" constant, $\lambda_{i,j}$ is the length of borderline between cell $i$ and its neighbors $j$. To prevent star flow anisotropies near the center of galaxy, which occur due to change in the length ratios of the cell sides, we correct corresponding $\lambda$ to keep star flows through each side of the cell equal.

The evolution of gas content in the cell $G_i$ is given taking into account SSP evolution:

$$\frac{\Delta G_i}{\Delta t} = -\Psi_i + A_i - \sum_j F_{i,j} - m_{\mathrm{OUT},i} + \sum_k \sum_l (S_i \circ R)_{k,l}, \qquad (5)$$

where $A_i$ is the accreted gas mass, $F_{i,j}$ are the gas mass flows (see section Gas flows) between cell $i$ and neighboring cells $j$, $m_{\mathrm{OUT},i}$ is the outflow from the disk (see section Gas outflows) and $R$ is the array representing the mass fraction of stellar populations returned to gaseous content, i.e., the last term[1] represents the total gas mass returned to gas pool of the cell $i$ by stellar populations evolving within this cell (the indices $k$

---

[1] Also known as Hadamard (or Schur) product, for two matrices of the same dimension, $(B \circ C)_{k,l} = B_{k,l} \cdot C_{k,l}$

and $l$ denote the age and metallicity, respectively).

The metallicity ($Z_i$) evolution of the gas content in the $i$-th cell is given by

$$\frac{\Delta(Z_i \cdot G_i)}{\Delta t} = -\Psi_i \cdot Z_i + A_i \cdot Z_A - \sum_j F_{i,j} \cdot Z_j - m_{\mathrm{OUT},i} \cdot Z_{\mathrm{OUT},i} + \sum_k \sum_l (S_i \circ Z)_{k,l}, \quad (6)$$

where $Z_A$ represents the metallicity of the accreting gas, $j$ denotes the neighboring cells, $Z_{\mathrm{OUT},i}$ is the metallicity of the outflowing gas, and $Z$ is the array representing yields of metals returned to the gas pool of the i-th cell by stellar populations evolving within this cell.

## 1.5. Gas flows

Due to the small size ($\sim 100 \times 100$ pc) of cells covering the galaxy disk, gas masses are expected to flow beyond the cells in one time step. The main structures causing gas movement are super-bubbles inflated by SF feedback. Following the formulation by Castor et al. (1975), on time-scale of 10 Myr super-bubbles reach $\sim 100$ pc in size for a typical gas density of $20\,M_\odot/\mathrm{pc}^2$ and SFE values of a few percent. Therefore, a cell experiencing a SF event on a time-scale of 10 Myr will be filled with hot tenuous gas, causing a large part of the gas to move out of the cell.

After 40 Myr, when supernovae vanish and the super-bubble inflated cavity cools down, the gas returns to the cell. The force driving the gas to refill the cell is the random motion of H I gas clouds. The refill timescale on 100 pc scales is assumed according to Roy & Kunth (1995), $\tau = 50\,\mathrm{Myr}$.

We implemented both types of gas flows in the galaxy disk model: expulsion by a SF event and refilling.

• *Gas expulsion*: this is implemented simply by moving gas from the cell $i$, experiencing a SF event, to the neighboring cells $j$. The gas flows only to those neighbors which have had no a SF event for the past 40 Myr:

$$F_{i,j} \cdot \Delta t = \lambda_{i,j} \cdot \begin{cases} 0 & \Delta_{\mathrm{SF},j} \leq 40\,\mathrm{Myr} \\ G_i & \Delta_{\mathrm{SF},j} > 40\,\mathrm{Myr}, \end{cases} \quad (7)$$

where gas flows between cells $F_{i,j}$ depend on the length, $\lambda_{i,j}$, of the borderline, and $G_i$ is the gas mass remaining in the cell $i$ after the SF event. The flow occurs within one time step after the SF event.

- *Gas refilling*: this is implemented under the assumption that equilibrium gas distribution in the galaxy follows the present-day baryonic matter distribution $B(r)$, i.e., any deviation from it, $G(r_i)/G(r_j) \neq B(r_i)/B(r_j)$, generates gas flows between cells on the time-scale $\tau$:

$$F_{i,j} = \lambda_{i,j} \cdot \frac{1}{\tau} \cdot \frac{G(r_j) \cdot B(r_i) - G(r_i) \cdot B(r_j)}{B(r_i) + B(r_j)}. \tag{8}$$

## 1.6. Gas outflows

When a super-bubble expands rapidly enough it accelerates to the escape velocity, i.e., a fraction of gas leaves the galactic gravitational potential. Outflows of gas from galaxy disks are important for the chemical evolution of galaxies. To simulate outflows from galaxy disks we implemented a model of expanding super-bubbles in stratified atmospheres following Baumgartner & Breitschwerdt (2013). We assume, that after SF event in a cell all newly formed supernovae explode in the center of the cell, which is located exactly at the mid-plane of the disk. We derive the mid-plane gas density assuming hydrostatic equilibrium condition and a constant along radius disk scale height, $h_z = 100 \, \text{pc}$. These approximations make the speed of the expanding super-bubble in the $z$ direction (perpendicular to the galaxy disk) dependent only on the gas density in the cell and the mass of newly formed stars (luminosity of the last stellar population).

Baumgartner & Breitschwerdt (2013) derived disk outflow conditions for the Milky Way by assuming that the expansion velocity of the top of super-bubble reaches a critical value, $v_{z,c} = 20 \, \text{km/s}$, before the acceleration (due to exponentially dropping gas density) in the $z$ direction begins. We applied the same critical value to the galaxy M33 models.

In our models we assume, that once outflow condition is fulfilled for the SF event, the cell loses gas instantly. We assume, that the gas lost from the cell is composed of the ejecta produced during the last $10 \, \text{Myr}$ from dying stars of all populations residing in it. Therefore, mass of gas lost from the cell $i$, $m_{\text{OUT},i}$, after a SF event is:

$$m_{\text{OUT},i} = \begin{cases} 0, & n_{\text{SN}} \leq f(\Sigma_{\text{G},i}) \\ \eta \cdot E_i, & n_{\text{SN}} > f(\Sigma_{\text{G},i}), \end{cases} \tag{9}$$

where $n_{\text{SN}}$ is an average number of supernovae expected from the SF event, $f(\Sigma_{\text{G},i})$ – Baumgartner & Breitschwerdt (2013) condition for the outflow, $E_i$ – returned gas

during the last 10 Myr from all populations residing in the cell, $\eta$ – a free parameter controlling fraction of the lost gas. If a SF event produces $n_{\mathrm{SN}} \leq 2$, the outflow from the cell is suppressed.

## 1.7. CMD generation

For each disk model cell we keep a complete star formation history in a matrix $S(t, Z)$ with age $t$ and metallicity $Z$ dimensions. The step in age dimension, $\delta t$, is equal to the model integration time step. The step in metallicity dimension varies in the range of $0.1-0.3$ dex. Each stellar population, corresponding to the particular matrix element, at birth is generated by using stochastically sampled initial mass function. We assume that stellar population $j$, corresponding to the matrix element $S(t_j, Z_j)$, has ages uniformly sampled within the time interval of $\delta t$. For each stellar population $j$ we find the nearest by age isochrone in the library and interpolate luminosity for each star from this population. However, we do not interpolate stellar luminosities among metallicities. See Table 1 for the parameters used to generate CMDs.

## 2. The M33 galaxy

In this section we discuss our stochastic 2-D galaxy disk evolution model applied to study the M33 galaxy disk (Mineikis & Vansevičius 2014a). We derived the M33 baryonic disk parameters from the galaxy rotation curve and used them to define the radial gas accretion profile in the model. For the M33 galaxy analysis we explored a grid of models constructed by varying the three most important parameters: $P_{\mathrm{T}}$, $\epsilon$, and $\alpha$. The grid was composed of 935 models: 17 values of $P_{\mathrm{T}}$, the linear step in the range $0.28 - 0.44$; $11 - \epsilon$, the logarithmic step in the range $0.018 - 5.7\,\%$; and $5 - \alpha$, the linear step in the range $1.5 - 2.5$. For simplicity we kept $\eta$ fixed, $\eta = 0$.

Comparisons of the models with observational data for the galaxy M33 are presented in Fig. 1. The models are compared with 1-D radial profiles of: gas surface density (H I from Corbelli & Salucci (2000), $H_2$ from Heyer et al. (2004), surface brightness in $i$ Ferguson et al. (2007) and GALEX $FUV$ (Muñoz-Mateos et al. 2007) passbands, and metallicity (Urbaneja et al. (2005); U et al. (2009)).

The gas surface density radial profile derived from observations constrains strongly the model parameter space due to large variation of the model gas density radial profiles, especially in the inner parts of the galaxy (Fig. 1, panel a).
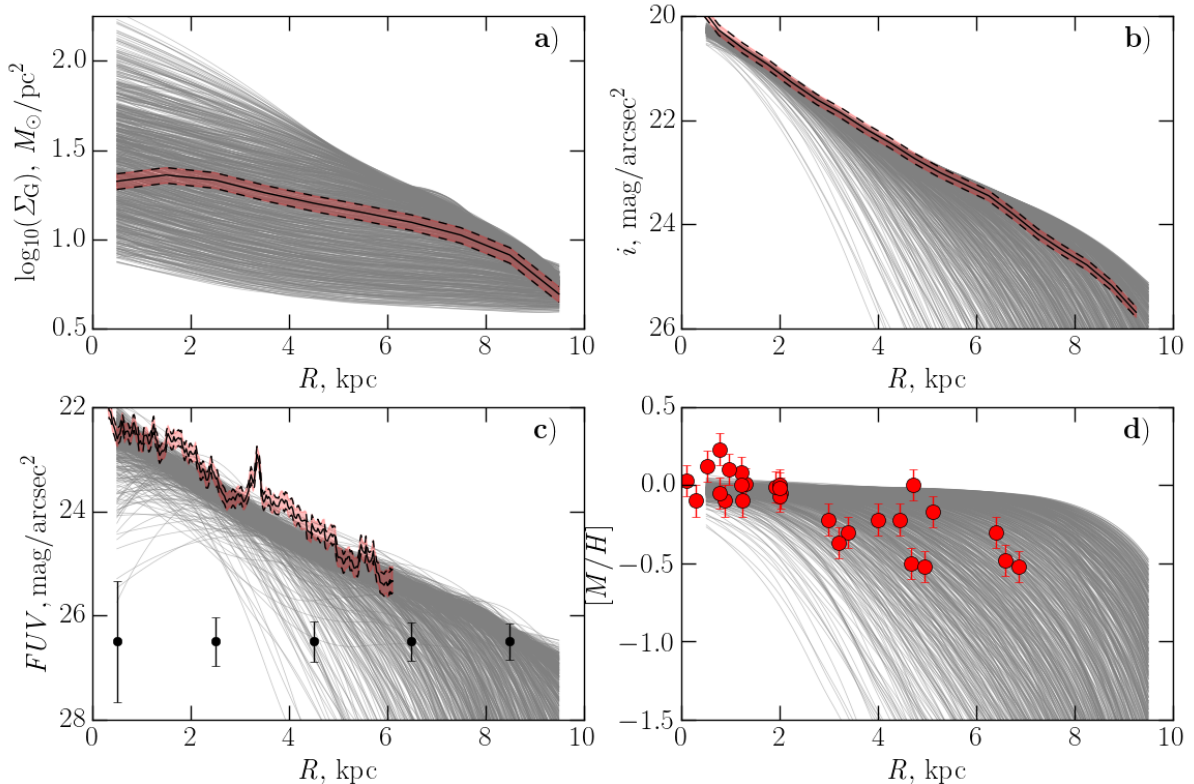
**Fig. 1.** Comparison of the observational data on the galaxy M33 with the models. The gas surface density (panel a) is computed by co-adding the radial profiles of H I (Corbelli & Salucci 2000) and H$_2$ (Heyer et al. 2004) gas surface density. The surface brightness radial profile in the $i$ passband (panel b) (Ferguson et al. 2007) is corrected for internal extinction using the radial extinction profile by Muñoz-Mateos et al. (2007) and assuming the LMC-like extinction law (Gordon et al. 2003). The surface brightness radial profile in GALEX $FUV$ passband (panel c) (Muñoz-Mateos et al. 2007) is also corrected for internal extinction. The metallicity measurements of blue super giant stars (panel d) are taken from Urbaneja et al. (2005) and U et al. (2009). All radial profiles of observed surface brightness are de-projected adopting 54° for the galaxy disk inclination.

The surface brightness radial profile in the $i$ passband constrains well the stellar mass of the models. However, we set the same total mass for all models, thus there are no significant variations in the $i$ passband radial profiles, except in the outer parts of the galaxy, where model radial profiles span a wide range (Fig. 1, panel b).

The GALEX $FUV$ passband surface-brightness radial profile constrains well the SF rate along the model galaxy radius (Fig. 1, panel c). However, this profile is not very sensitive to the model parameters since the accretion time-scale exceeds the gas consumption time-scale, i.e., SF is gas-accretion regulated (Elmegreen 2015, and references therein).

The metallicity radial profiles (Fig. 1, panel d) are sensitive to the model parameters, however, their use is limited due to large scatter in the observational data.
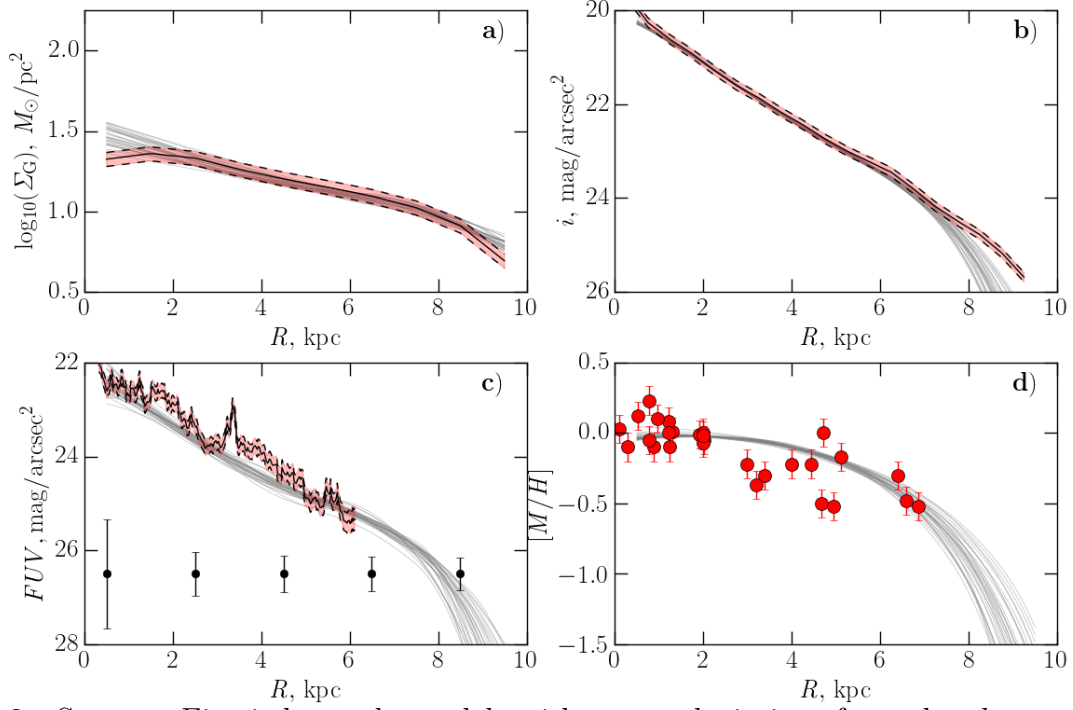
**Fig. 2.** Same as Fig. 1, but only models with r.m.s. deviations from the observed radial profiles (gas surface density and $i$ passband) smaller than 10% and in the radial distance range 2–7 kpc are shown.
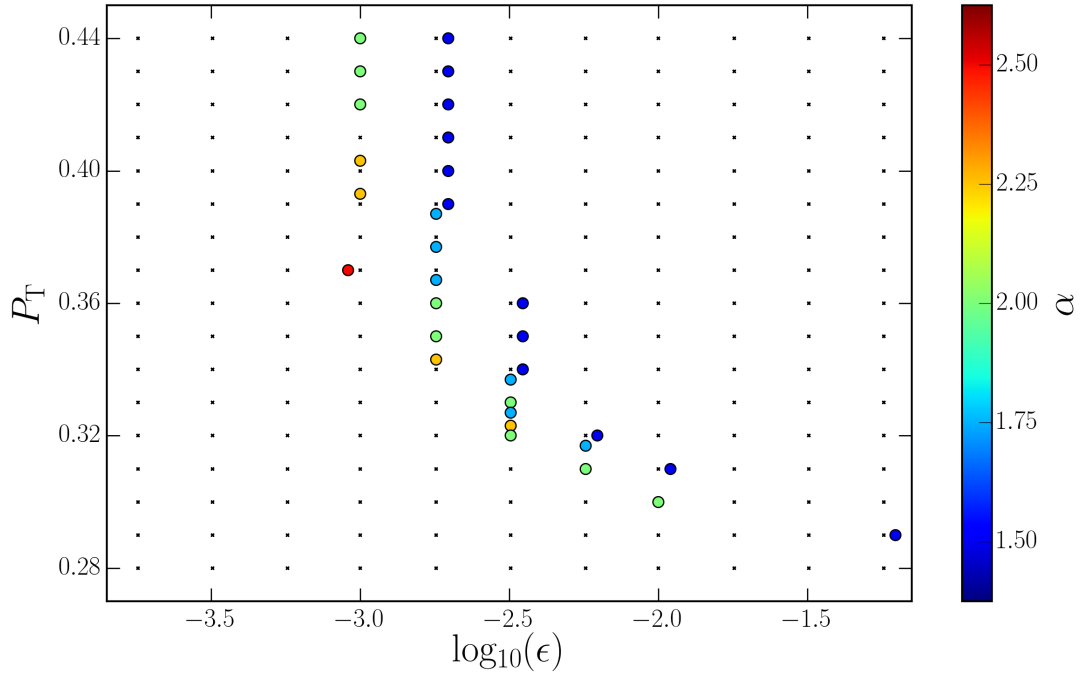


**Fig. 3.** 3-D parameter space of the models shown in Fig. 2. The colored circles indicate the values of $\alpha$ parameter. The small black points at each node of the model grid indicate a fully explored extent of the parameter space.
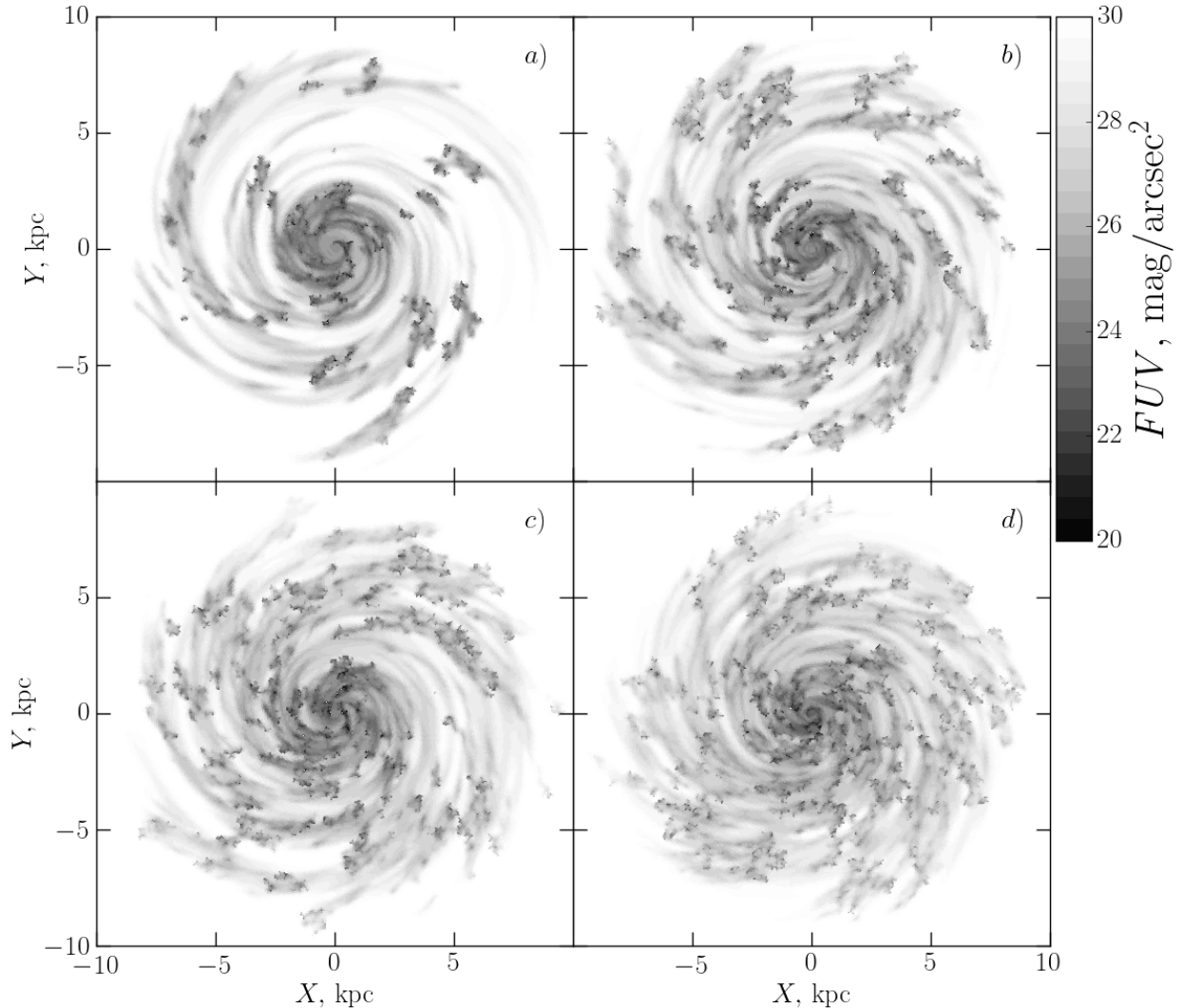
**Fig. 4.** The galaxy models from the "degeneracy valley" (Fig. 2) in the GALEX *FUV* passband: (a) $P_{\mathrm{T}} = 0.30$, $\epsilon = 1\%$; (b) $P_{\mathrm{T}} = 0.31$, $\epsilon = 0.6\%$; (c) $P_{\mathrm{T}} = 0.32$, $\epsilon = 0.3\%$; (d) $P_{\mathrm{T}} = 0.34$, $\epsilon = 0.2\%$. For all models, $\alpha = 2$. The models possess very similar 1-D radial profiles, but they demonstrate different 2-D patterns of the young SF regions.

Therefore, to further constrain the model parameter space we used only the gas surface density and the $i$ passband radial profiles. For each model we calculated the r.m.s. deviations from both observed radial profiles in the most reliable (for models) radial distance range, i.e., 2–7 kpc. The inner region of the model galaxy has an increasingly anisotropic grid and the outer parts are affected by the uncertainty in the critical gas surface density, $\Sigma_{\mathrm{C}}$. In Fig. 2 we show the models selected by r.m.s. deviations from the observed radial profiles (gas surface density and $i$ passband) being less than 10%.

The parameter space of the selected models is shown in Fig. 3. A prominent feature of this figure is the "degeneracy valley" – the region in the parameter space where

reside the models selected by the 1-D radial profile procedure described above. The "degeneracy valley" forms because the 1-D radial profiles are derived by convolving the 2-D distributions of SF regions, e.g., SF in the model galaxy being smooth and inefficient or patchy and efficient would produce similar 1-D radial profiles. This effect is seen in Fig. 4, where four different models taken from the "degeneracy valley" are plotted, i.e., by increasing $P_{\mathrm{T}}$ and decreasing $\epsilon$ values we make SF more smooth.

To demonstrate how to break the degeneracy of the parameters, we selected three models from the "degeneracy valley" with $P_{\mathrm{T}}$ and $\epsilon$: 0.3 & 1 % (model A); 0.34 & 0.2 % (model B), and 0.44 & 0.1 % (model C). We used models with constant $\alpha = 2$ and varied $\eta$ in the range $0.2 - 0.9$. Even with identical $\eta$ values, the models lose different amounts of metal-enriched gas because of the different SF efficiency.

The models with the highest $\epsilon$ experience more massive SF events which are capable to produce outflows even in the outer regions of disks. In contrast, the models with lowest $\epsilon$ values form less massive stellar populations, i.e., cells lose smaller amount of the enriched gas. The radial profiles of the enriched gas loss also differ between the models. In the central parts of the galaxy all models lose similar fraction of the enriched gas, however, in the outer parts difference is more pronounced. The highest $\epsilon$ models lose significantly more metals in the outer parts compared to the lowest $\epsilon$ models. Therefore, differences in the metal enrichment history of the models make it possible to break the parameter degeneracy.

However, to constrain galaxy SF parameters, the resolved stellar photometry is necessary. For the CMD analysis we used the HST/ACS WFC stellar photometry data in four fields within the galaxy M33, kindly provided by Benjamin Williams (Williams et al. 2009).

The sizes of areas, used to sample models at different radial distances, are the same as those of areas measured in Williams et al. (2009). To compare the model and observed CMDs we adopt for M33 a distance of 840 kpc, the same extinction for all fields, $A_V = 0.3$, and apply to the model stars Gaussian errors calculated using the relation between photometric errors and magnitude, which was derived from the observed star catalog individually for each field. The extinction for the HST/ACS bands was calculated according to Cardelli et al. (1989), with $R_V = 3.1$. Note, however, that in estimating the errors we do not take into account the effects of crowded field photometry and differential extinction within the galaxy M33.

In Fig. 5 we plotted CMDs of the model A with different values of the outflow parameter $\eta$, together with the observational data for M33. The model CMDs with
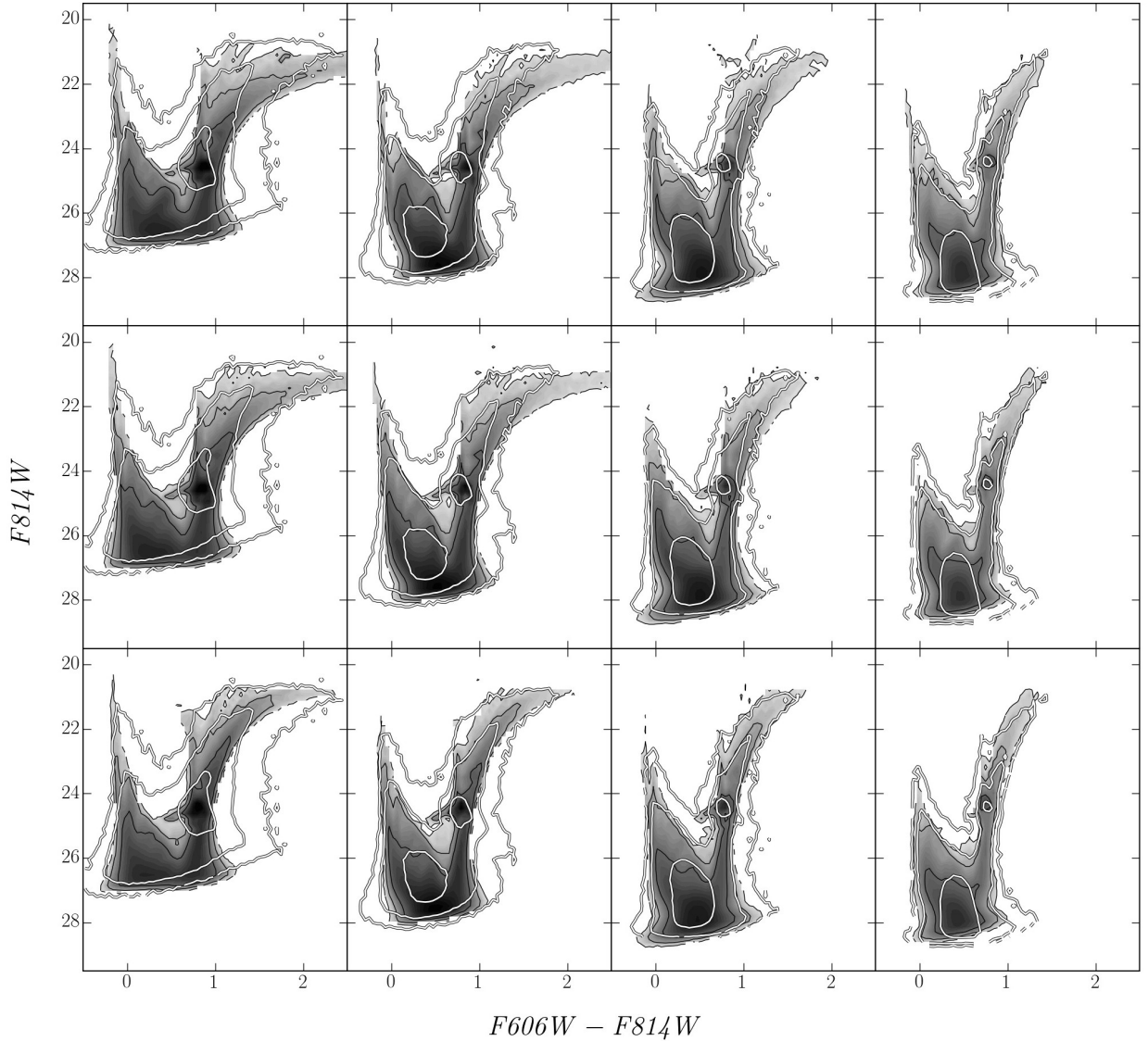
**Fig. 5.** HST/ACS WFC resolved stellar photometry data of the galaxy M33 (Williams et al. 2009). The contour lines represent observed CMD star density in the logarithmic scale (adjacent lines indicate density differing by 10) compared with the model A CMDs star density plotted in grey (logarithmic scale). In the top panel row model CMDs with $\eta = 0.2$, middle – $\eta = 0.5$, and bottom – $\eta = 0.9$ are plotted. The panel columns from the right to the left show CMDs sampled at 0.9, 2.4, 4.1, and 5.8 kpc radial distances from the galaxy M33 center.

$\eta = 0.2, 0.5, 0.9$ are shown in the top, middle, and bottom rows of panels, respectively. The model CMDs sampled at different distances from the galaxy center, 0.9, 2.4, 4.1, and 5.8 kpc, are shown in the columns of panels from the left to the right, respectively. Fig. 5 shows that CMDs of the model A are incompatible with the M33 data. With $\eta = 0.2, 0.5$, only the CMDs in the outermost fields match the observations. The inner fields display features of clearly too metallic stellar populations in comparison with the observed data. The model CMDs with the highest value of the outflow
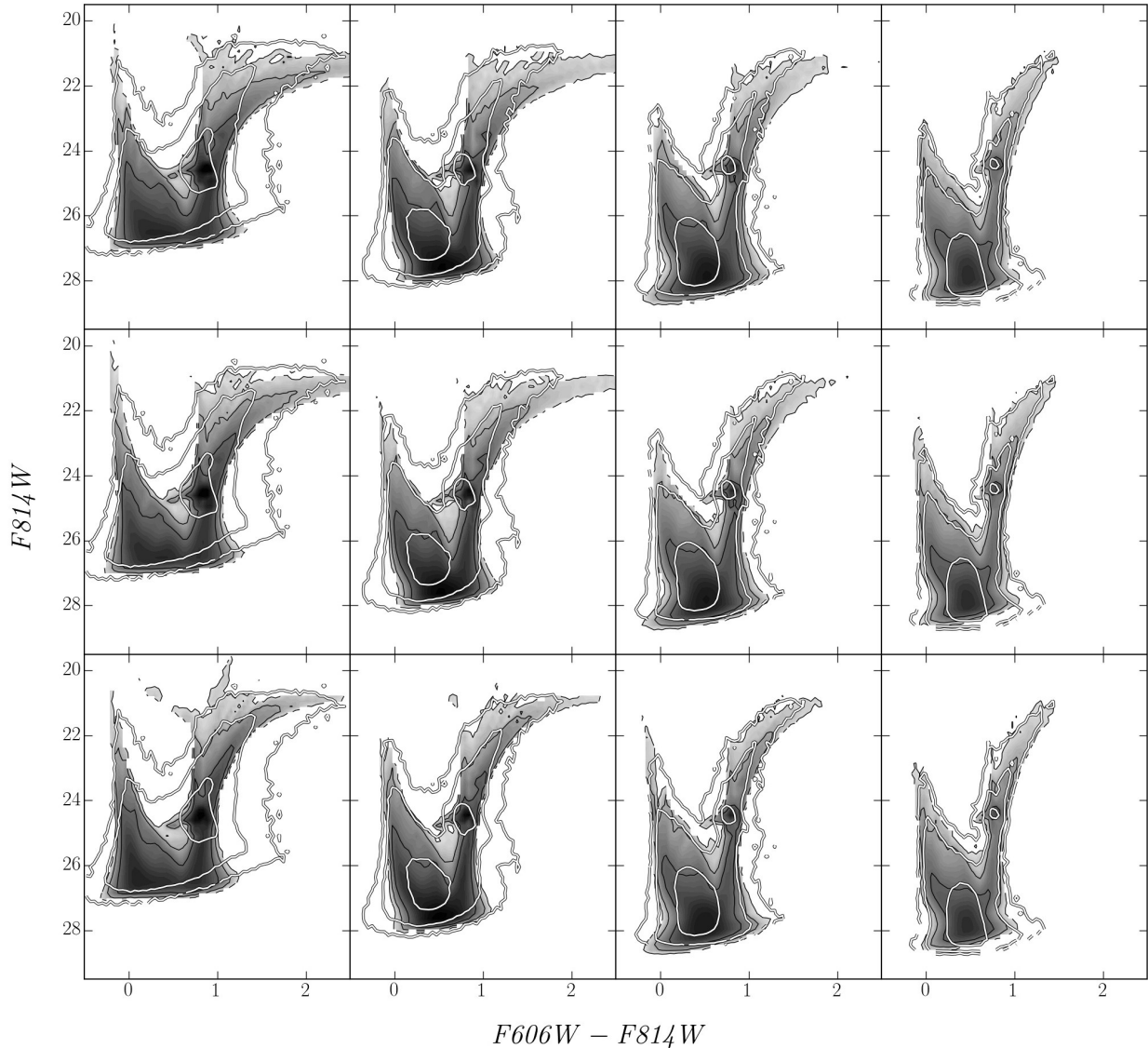
**Fig. 6.** The same as in Fig. 5, but for the model B.

parameter, $\eta = 0.9$, in the inner fields match the observational data, however, in the outer fields, the models are clearly too metal deficient.

In Fig. 6 we compare, in a similar way, the observations with the model B. In the cases of $\eta = 0.2, 0.5$ we see, again, the CMD features of too metallic stellar populations in the inner fields. However, contrary to the model A, in the case of $\eta = 0.9$ (bottom row of panels), the CMDs of the model B match the observations both in the inner and in the outer fields.

The model C with the lowest value of $\epsilon$ is compared with the observations in Fig. 7. The low values of $\epsilon$ suppress gas outflow from the galaxy due to relatively low-mass stellar populations forming in the disk. As a result of this effect, even models with highest $\eta$ values shows too metallic stellar populations throughout the galaxy disk.
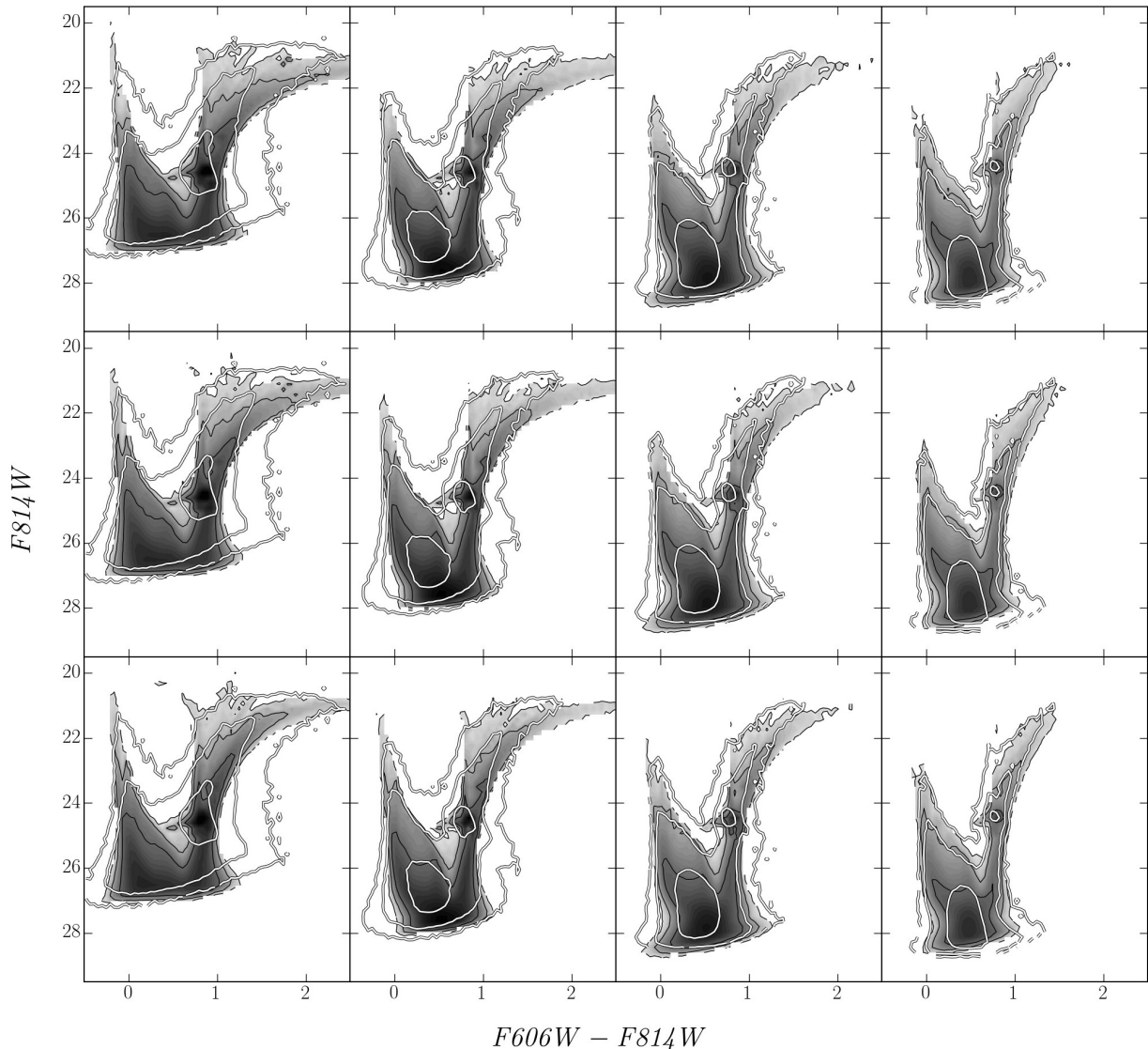
20

**Fig. 7.** The same as in Fig. 5, but for the model C.

# 3. Models of the late-type disk galaxies: 1-D versus 2-D

In this section we compare our stochastic 2-D galaxy disk evolution model with the smooth SF 1-D model (Mineikis & Vansevičius 2014b). The 1-D model used for the comparison is constructed following the approaches developed for the nearby disk galaxies, e.g., Marcon-Uchida et al. (2010). The model is defined by dividing disk into concentric rings of 1 kpc in width. The disk grows by a gradual gas accretion from the reservoirs (assigned to each ring) where gas resides initially. The gas does not migrate in the radial direction and always is well mixed. The individual evolution of each ring is computed by using the package PEGASE-HR (Le Borgne et al. 2004) and the Schmidt-Kennicutt type SF law (Kennicutt 1989):

**Table 2.** Parameters of the 2-D models used for the comparison.

| Model | $P_{\mathrm{T}}$ | $\epsilon$, % | $\alpha$ |
|---|---|---|---|
| High stochasticity (HS) | 0.30 | 1.0 | 2 |
| Low stochasticity (LS) | 0.34 | 0.2 | 2 |

$$\mathrm{SFR}_i = \frac{1}{\tau_{\mathrm{SF},i}} \cdot \left( \frac{\Sigma_{\mathrm{G},i}(t)}{\Sigma_{0,i}} \right)^n, \tag{10}$$

where SF rate in the ring $i$, $\mathrm{SFR}_i$, is proportional to the gas density $\Sigma_{\mathrm{G},i}$ normalized by the initial reservoir mass density $\Sigma_{0,i}$; the star formation parameter $\tau_{\mathrm{SF},i}$ defines the time-scale of the galaxy ring build up. The PEGASE-HR parameters used to generate 1-D and 2-D models are given in Table 1.

To compare 1-D and 2-D model predictions, we derived SF prescription for the 1-D models from the 2-D models fitted for the M33 galaxy. The 1-D model SF is based on the Schmidt-Kennicutt law and is controlled via two parameters, $n$ and $\tau_{\mathrm{SF}}$. We used the parameter $n = 3$ derived from the observations (Heyer et al. 2004). The $\tau_{\mathrm{SF},i}$ parameter values for each ring were derived from the 2-D low stochasticity models (LS, see Table 2) by equation (10).

We succeeded to calibrate the smooth SF 1-D models and transform them to the system common to the stochastic SF 2-D models. Therefore, by comparing the evolution of the main SF parameters for both models, we were able to clearly demonstrate the large effects arising due to SF stochasticity, see Fig. 8 for the case of LS model.

We do not see strong stochasticity effects on the gas surface density and metallicity evolution. However, the effect of these parameters on the SF rate at the early ages is evidenced by strong discrepancy between the 1-D and 2-D models. This effect appears due to a low gas surface density, which is insufficient for normal self-propagating SF in the 2-D models. A huge scatter in the SF rate is prominent, being the largest in the central regions and outskirts of the galaxy disk. In the central disk regions the scatter is partly caused by a smaller number of cells forming the ring 1 kpc wide. In the disk outskirts the scatter is large because the low gas density prevents the steady self-propagating SF.

Even stronger stochasticity effects on the SF rate are seen in Fig. 9 in the case of the 2-D models of high stochasticity (HS, see Table 2). The smooth SF 1-D models, shown in all figures, are calibrated only versus the LS models, because the differences between the LS and HS calibrations are small.
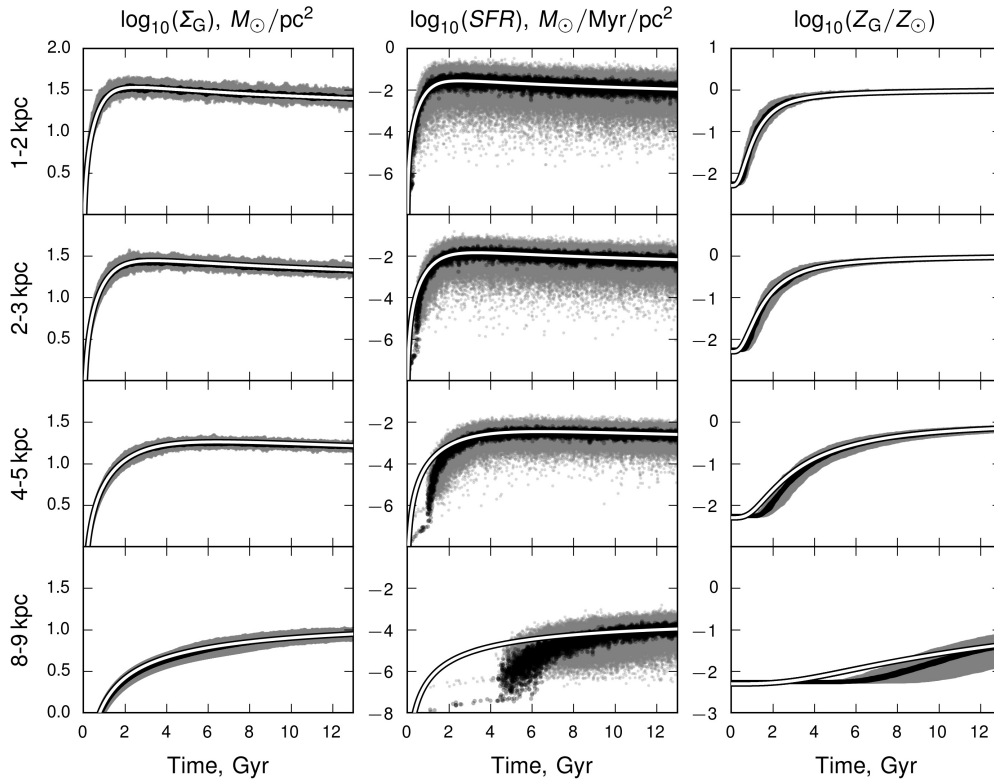
**Fig. 8.** The evolution of the gas & SF surface density and gas metallicity in radial rings. The white line indicates 1-D models. The black dots represent 8 independent runs of the LS model averaged within 1 kpc wide rings, the gray dots are for 0.1 kpc wide rings.
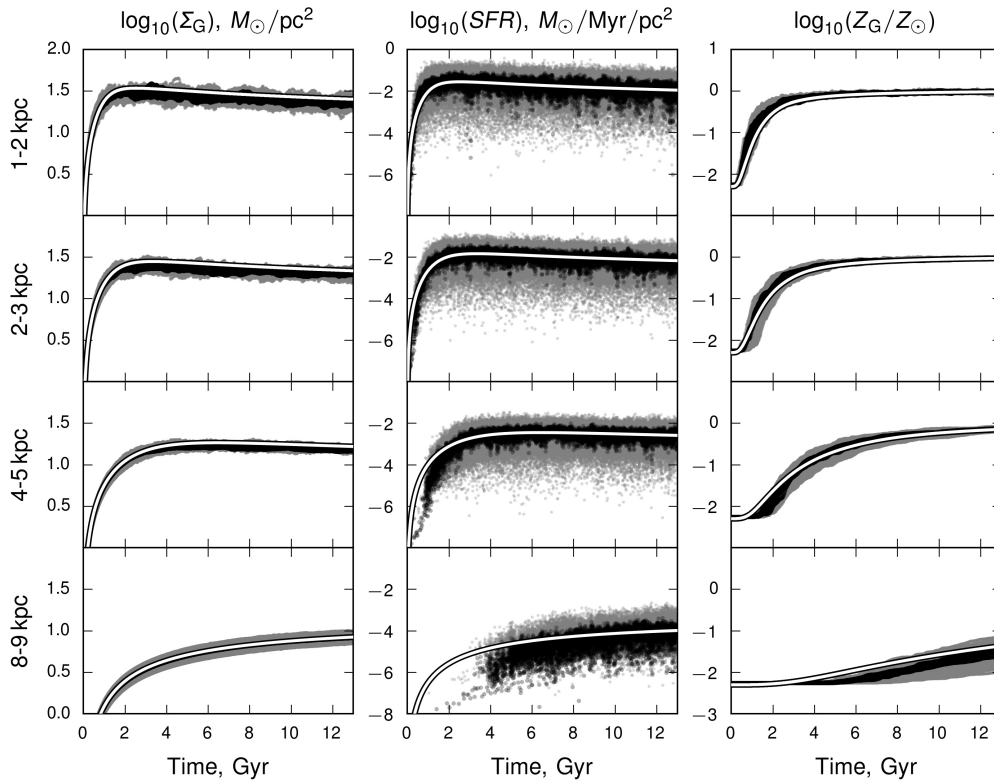


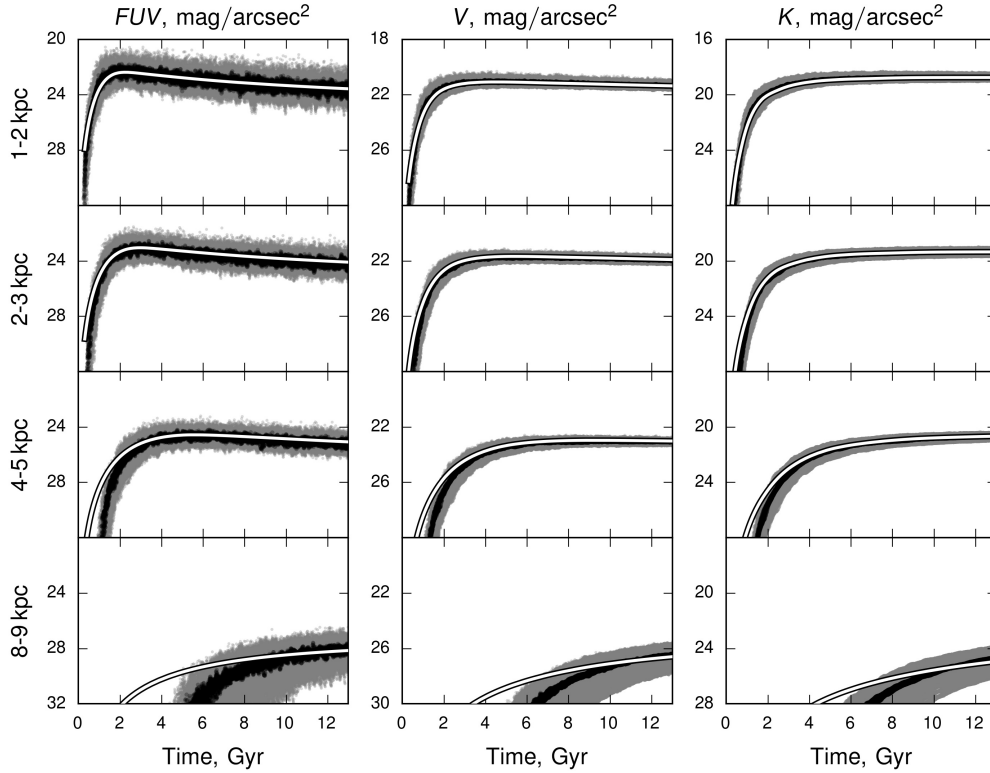**Fig. 9.** The same as in Fig. 8, but for the HS model.

**Fig. 10.** The same as in Fig. 8, but for the surface brightness in the GALEX *FUV*, *V* and *K* passbands.
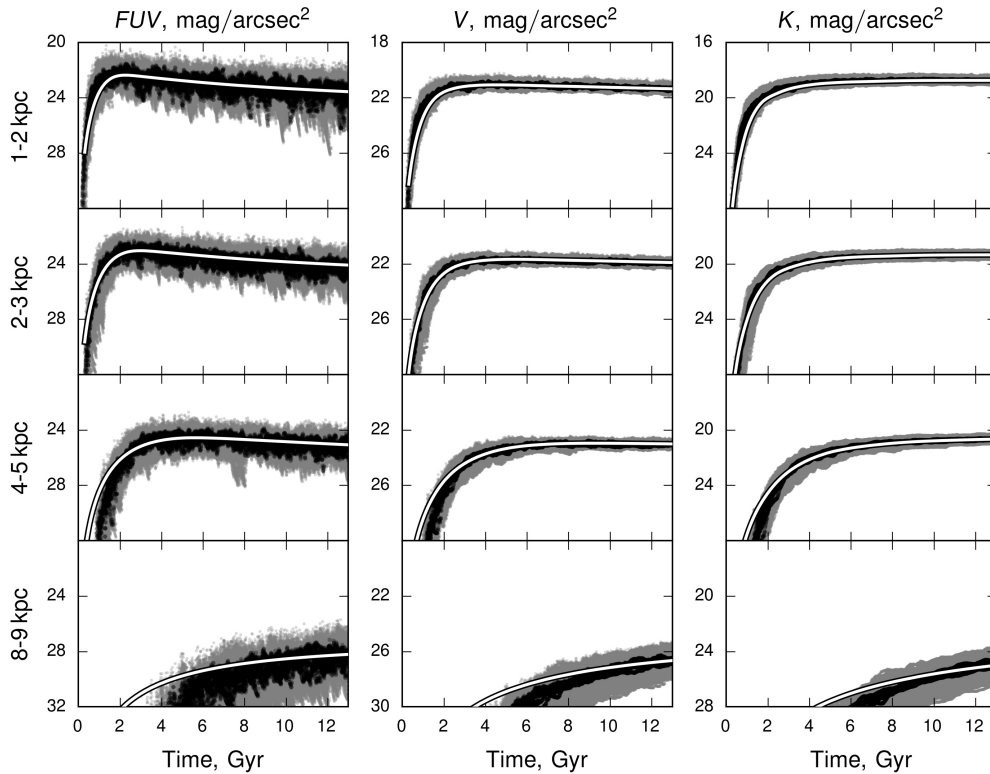


**Fig. 11.** The same as in Fig. 10, but for the HS model.

It is well known that spectral energy distributions of stellar populations are very sensitive to the bursting SF. The evolution of the surface brightness in the GALEX

*FUV*, *V* and *K* passbands at different distances from the galaxy center, averaged within rings 1 kpc wide, are shown in Fig. 10 (LS) and Fig. 11 (HS). Naturally, the largest stochasticity effects are seen in the GALEX *FUV* passband. In the outskirts of the disk, however, a large scatter is seen even in the *V* and *K* passbands.

## Conclusions

We proposed and tested the stochastic 2-D galaxy disk evolution model. The star formation in the model is simulated as a stochastic self-propagating process. Additionally, parameterized gas and stars flows in the disk and metal enriched gas outflows from a galaxy are taken into account. The software package developed for the model enables to study 2-D chemical and spectrophotometric gas and stellar population evolution. The important feature of the model – ability to generate synthetic colour-magnitude diagrams of the resolved stellar populations at any position in a disk and for any time-step.

We applied the model to study the M33 galaxy disk evolution and successfully reproduced the main observational data – radial profiles of: surface gas density, metallicity, surface brightness in *FUV* and *i* passbands, as well as colour-magnitude diagrams along the major axis of the galaxy. We demonstrated, that using only radial profiles of the observational data it is not possible to fully constrain the model parameters due to degeneracy effects. In order to break the parameter degeneracy it is necessary to use 2-D capabilities of the model and synthetic colour-magnitude diagrams. The derived model parameters for the M33 disk: triggered star formation probability $P_\mathrm{T} = 0.34$, star formation efficiency $\epsilon = 0.2\,\%$, and metal enriched gas outflow $\eta = 0.9$.

We compared our stochastic 2-D galaxy disk model results with the smooth star formation 1-D galaxy disk evolution models, described by the empirical Schmidt-Kennicutt law. The 2-D model, being on average consistent with the 1-D model, shows large variations of star formation rate and surface photometric parameters, especially in the UV range, across the disk and in time. The largest stochasticity effects are predicted to occur in the central regions and outer parts of the galaxy disk during the first $1-2$ Gyr from the beginning of galaxy formation.

Our model and software developed to analyze the M33 galaxy disk evolution could easily be applied to study the nearby galaxies possessing the resolved stellar photometry data.

# References

Bastian N., Ercolano B., Gieles M., et al. 2007, MNRAS, 379, 1302

Baumgartner V., Breitschwerdt D. 2013, A&A, 557, A140

Cardelli J.A., Clayton G.C., Mathis J.S. 1989, ApJ, 345, 245

Castor J., McCray R., Weaver R. 1975, ApJ, 200, L107

Corbelli E., Salucci P. 2000, MNRAS, 311, 441

Elmegreen B.G. 2015, in Proceedings, Conference on Lessons from the local group (Springer), 477–488

Fakhouri O., Ma C.P., Boylan-Kolchin M. 2010, MNRAS, 406, 2267

Feitzinger J.V., Glassgold A.E., Gerola H., et al. 1981, A&A, 98, 371

Ferguson A., Irwin M., Chapman S., et al. 2007, in Proceedings, Conference on Island Universes: The Structure and Evolution of Disk Galaxies, 239–244

Gordon K.D., Clayton G.C., Misselt K.A., et al. 2003, ApJ, 594, 279

Guedes J., Callegari S., Madau P., et al. 2011, ApJ, 742, 76

Heyer M.H., Corbelli E., Schneider S.E., et al. 2004, ApJ, 602, 723

Kang X., Chang R., Yin J., et al. 2012, MNRAS, 426, 1455

Kennicutt Jr. R.C. 1989, ApJ, 344, 685

Kroupa P. 2002, Science, 295, 82

Le Borgne D., Rocca-Volmerange B., Prugniel P., et al. 2004, A&A, 425, 881

Marcon-Uchida M.M., Matteucci F., Costa R.D.D. 2010, A&A, 520, A35

McBride J., Fakhouri O., Ma C.P. 2009, MNRAS, 398, 1858

Mineikis T., Vansevičius V. 2010, Baltic Astronomy, 19, 111

—. 2014a, Baltic Astronomy, 23, 209

—. 2014b, Baltic Astronomy, 23, 221

Muñoz-Mateos J.C., Gil de Paz A., Boissier S., et al. 2007, ApJ, 658, 1006

Roškar R., Teyssier R., Agertz O., et al. 2014, MNRAS, 444, 2837

Roy J.R., Kunth D. 1995, A&A, 294, 432

Scannapieco C., Wadepuhl M., Parry O.H., et al. 2012, MNRAS, 423, 1726

U V., Urbaneja M.A., Kudritzki R.P., et al. 2009, ApJ, 704, 1120

Urbaneja M.A., Herrero A., Kudritzki R.P., et al. 2005, ApJ, 635, 311

Williams B.F., Dalcanton J.J., Dolphin A.E., et al. 2009, ApJ, 695, L15

Woosley S.E., Weaver T.A. 1995, ApJS, 101, 181

# Santrauka

Žvaigždėdaros procesų supratimas galaktikose yra vienas svarbiausių šiuolaikinės astrofizikos uždavinių. Nepaisant sparčiai augančio stebėjimų duomenų, tinkamų žvaigždėdaros tyrimams galaktikose, kiekio vis dar nėra greitų ir patikimų skaitmeninių modelių šiems duomenims analizuoti. Todėl mes sukūrėme stochastinį 2-D galaktikų diskų evoliucijos modelį. Jame žvaigždėdara modeliuojama kaip stochastinis saviindukcinis procesas. Papildomai modelyje įskaitomas dujų bei žvaigždžių judėjimas galaktikos diske ir sunkiaisiais elementais praturtintų dujų netekimas iš galaktikos. Modelis yra išskirtinis tuo, jog gali generuoti sintetines žvaigždžių populiacijų spalvos-ryškio diagramas bet kuriuo evoliucijos momentu ir bet kurioje galaktikos disko vietoje. Mūsų sukurtas programinis paketas modeliui realizuoti įgalina registruoti cheminę ir spektrofotometrinę 2-D informaciją per visą galaktikos evoliucijos laikotarpį.

Naują žvaigždėdaros modeliavimo galaktikose modelį panaudojome M33 galaktikos tyrimui. Remiantis detalia šios galaktikos evoliucijos analize buvo įrodyta, kad norint išspręsti galaktikos evoliucinių parametrų išsigimimo problemą būtina panaudoti ir 2-D galaktikos modelį, ir jo generuojamas spalvos-ryškio diagramas, kurios yra bene pati informatyviausia priemonė tiriant artimų galaktikų evoliuciją.

# Tadas Mineikis

*Curriculum Vitae*

| | | |
|---|---|---|
| **Date and place of birth:** | 1985 April 11, Lithuania | |
| **E-mail:** | tadas.mineikis@ftmc.lt | |

**Education:**

| | | |
|---|---|---|
| *B.S.* | in Physics at Vilnius University | 2008 |
| *M.S.* | in Physics, Theoretical Physics and Astronomy at Vilnius University | 2010 |
| *Ph.D. studies* | in Physical Sciences, Physics (02 P) at Vilnius University | 2010-2014 |

**Professional improvement:**

- *4th Lithuanian astronomical union conference, Lithuania, 2008*
- *38th National Lithuanian physics conference, Lithuania, 2009*
- *EstSpace School: Future Cosmic Surveys and Huge Databases, Estonia, 2009*
- *EuroVO-ICE School, France 2011*
- *39th National Lithuanian physics conference, Lithuania, 2011*
- *Saas Fee Course: Dynamics of Young Star Clusters and Associations, Switzerland, 2012*
- *Nordic Millimetre and Optical/NIR Astronomy Summer School: Observational cosmology and the formation and evolution of galaxies, Sweden, 2012*
- *Conference: European Week of Astronomy and Space Science, Finland, 2013*
- *Conference: Physical Processes of Galaxy Formation: Consensus and Challenges, France, 2013*